The elastic constants and related properties of β-HMX determined by Brillouin scattering

Lewis L. Stevens and Craig J. Eckhardt[a)]
Department of Chemistry, Center for Materials Research and Analysis, University of Nebraska–Lincoln, Lincoln, Nebraska 68588-0304

(Received 17 June 2004; accepted 8 February 2005; published online 29 April 2005)

By scattering from a variety of acoustic phonons, a complete stiffness tensor has been determined for crystalline β-HMX. The results are compared with recent experimental and theoretical determinations of the elastic constants and bulk modulus. Reasons for disagreement are discussed in terms of experimental limitations and anharmonic effects. The observed ordering of stiffness constants, C_{11} (18.4 GPa), C_{22} (14.4 GPa), and C_{33} (12.4 GPa), is qualitatively associated with physical phenomena including cleavage planes, patterns in crystal growth, and molecular packing. This interpretation is further corroborated by the linear compressibilities plotted in three crystallographic planes. The Voigt–Reuss–Hill bulk and shear moduli were found to be 9.9 and 3.7 GPa, respectively. The elasticity of β-HMX is also discussed in relation to proposed mechanisms for the initiation of detonation. © *2005 American Institute of Physics*. [DOI: 10.1063/1.1883627]

INTRODUCTION

The structure-function relationship for many materials remains a fundamental question in solid-state research. Concomitant with a broader understanding of this relationship, the properties of solid-state materials are becoming increasingly tunable.[1–3] This comprehension, particularly for the mechanical properties, is essential to the development of secondary explosives, such as HMX (cyclotetramethylenetetranitramine), that characteristically balance low sensitivity to detonation with high power. Elasticity is fundamental to understanding such materials' mechanical response to stress. The elastic constants, which arise from intermolecular forces, provide a window into the microscopic interactions that affect phonon propagation, lattice compressibility, and thermal conductivity. A well-developed experimental basis, particularly for elasticity, not only provides insight into the fundamental cohesive forces of solids but also allows construction of theoretical potentials that more accurately reproduce and predict the properties of materials.

A detailed understanding of the mechanical properties can also provide insight into solid-state reactivity. The original picture of organic solid-state reactivity was developed using the topochemical principle.[4] However, as more organic systems were studied, application of this principle became increasingly limited. Evidence for an active role of the lattice led to an extended, analytical development of a model for solid-state reactivity.[5,6] This model incorporates local strain fields and cooperative effects such as exciton–phonon or phonon–phonon coupling. Strain fields have been proposed to be fundamental to understanding the photochemically induced, solid-state reactions observed in diundecanoyl peroxides[5] and 2,5-distyrylpyrazine (DSP).[6] In the context of strain-mediated solid state reactivity, mechanochemical transformations, such as detonation, are a natural branch of solid-state reactions. While the phenomenon of detonation is well known, the initial mechanism by which mechanical energy becomes available for molecular dissociation, other than by thermalization, is not.[7] Insight into the mechanisms of detonation is limited due to the complicated spatial and temporal regimes associated with different stages of detonation. However, our focus is with the *initial* shockwave-induced molecular response, i.e., on the femtosecond time scale. Since the shockwave traverses, at least initially, an intact lattice, the solid's mechanical properties are particularly germane to understanding the material's response to this initial step of detonation.

The goal of this research is to experimentally determine a complete stiffness tensor for β-HMX. This ambient pressure- and temperature-stable polymorph crystallizes in the monoclinic system.[8,9] As a consequence of this low symmetry, 13 elastic constants are required to fully describe the molecular displacements associated with an arbitrary elastic wave. This significantly complicates the experimental determination of a complete stiffness tensor. These complications have, in part, led to a lack of experimental data and of consistency among the relatively few stiffness tensor determinations for molecular crystals, most of which are of low symmetry. Zaug has reported the first experimentally determined stiffness tensor for β-HMX.[10] However, due to limited sample orientations, only five elastic constants were experimentally accessible. While his work provides a first step toward a better understanding of the mechanical properties of β-HMX, a complete picture of its elasticity can only be drawn if all elastic constants are experimentally determined.

A variety of theoretical methods and potentials have been used to successfully calculate the lattice parameters and heat of sublimation for β-HMX.[11–14] While these methods are becoming increasingly competent at reproducing the static properties, the more potential-sensitive dynamical

[a)]Author to whom correspondence should be addressed. Electronic mail: eckhardt@unlserve.unl.edu

properties have not been as widely investigated. Sewell *et al.* have reported two separate calculations of the stiffness tensor using the same quantum-chemistry-based force field in different types of molecular simulations.[15,16] The earlier reported elastic constants were calculated from a molecular-dynamics (MD) simulation based on the Rahman–Parrinello isothermal–isobaric (*NpT*) approach. The authors note that determining the elastic tensor using this method, which used an external barostat coupled to the lattice through the stress tensor, is disadvantageous due to the sensitivity of this coupling. This complication, coupled with a lower than expected isothermal bulk modulus of 11.1 GPa, prompted a new method of calculation. The second approach used an isothermal–isochoric MD simulation coupled with a permutation of the cell and its volume with an *NpT* Monte Carlo method. This calculation produced a significantly less compliant lattice for β-HMX. Such discrepancies in the calculated results require resolution by experiment.

In the next following sections, a brief introduction to Brillouin scattering is given. All 13 elastic constants of β-HMX are then presented and compared to the results of earlier work. This is followed by a discussion of some specific elastic constants and linear compressibilities. Finally, the role of elasticity with emphasis on shear deformation in recently developed models for detonation is discussed.

THEORY

The theory of Brillouin scattering is well documented.[17,18] Near the Brillouin-zone center, the wavelength of an acoustic phonon is on the order of hundreds of unit cells. This mesoscopic scale permits modeling the material as an elastic continuum with a propagating acoustic wave described by

$$\rho \ddot{u}_i = c_{ijkl} \frac{\partial^2 u_l}{\partial r_j \, \partial r_k}, \tag{1}$$

which relates the density ρ and the ith component of the molecular displacement about the equilibrium position u_i to its spatial derivatives through the elastic coefficient tensor c_{ijkl}. Substituting a plane-wave solution into Eq. (1) and using the long-wavelength approximation yield

$$\left(c_{ijkl} q_k q_l - \rho \nu^2 \delta_{im}\right) u_m^0 = 0, \tag{2}$$

in which the $q_{k,l}$ are the appropriate direction cosines representing the phonon $\mathbf{q}$ referenced to a Cartesian system. Nontrivial solutions arise from the Christoffel determinant,

$$\left| c_{ijkl} q_k q_l - \rho \nu^2 \delta_{im} \right| = 0, \tag{3}$$

whose eigenvalues are related to the three acoustic velocities for an arbitrary $\mathbf{q}$. The polarization of the three acoustic modes is often mixed. Therefore, for each $\mathbf{q}$ there are two quasitransverse modes, often differentiated as slow and fast quasitransverse modes, and one quasilongitudinal mode. When the elastic constants are not known, an overdetermined set of experimental velocities can be used to calculate them from Eq. (3).

As an acoustic phonon travels through the lattice, the molecular displacements generate a periodic fluctuation in the local density. Bragg reflection from this "thermal grating" gives rise to the Doppler-shifted frequencies observed in Brillouin scattering. The acoustic velocities are then calculated from these frequency shifts using the Brillouin shift equation for an optically anisotropic medium,

$$\delta\omega_e = \pm \frac{\nu_e \omega_i}{c} \sqrt{n_i^2 + n_s^2 - 2 n_i n_s \cos\theta}, \tag{4}$$

where n_i and n_s represent, respectively, the refractive indices of the crystal along the incident and scattered light directions, θ is the angle between these directions, $\delta\omega_e$ is the angular frequency shift relative to the incident angular frequency ω_i, and ν_e is the acoustic velocity. From these velocities, the elastic constants are determined using an iterative, linear, least-squares minimization routine.[19] The minimization routine incrementally steps the elastic constants until a minimum in the square of an error vector is found,

$$e^T e = \sum_j \left| \rho \nu_{e,j,\mathrm{obs}}^2 - \rho \nu_{e,j,\mathrm{calc}}^2 \right|^2. \tag{5}$$

This minimum represents the set of elastic constants that most accurately reproduces the experimental data.

EXPERIMENT

Crystal parameters

Optical quality, untwinned, single crystals of β-HMX were evaporatively grown from an acetone solution held at 20 °C. The $P_{2_1/n}$ space group and lattice parameters were verified using x-ray diffraction and were consistent with those reported by Kohno *et al.*[9] The crystals exhibited well-formed faces predominately zonal to the *a*-crystallographic axis. In order to assign the faces, the angles between all zonal and capping faces were determined by optical goniometry. The indices, which were subsequently corroborated by single-crystal x-ray diffraction, are necessary to precisely define the scattering angle θ.

In addition to a well-defined scattering geometry, the refractive indices must be determined in order to solve Eq. (4). For β-HMX, the axes of the optical indicatrix are not constrained by symmetry to be coincident with all crystallographic axes. The principal directions for each unique face were determined with near-normal-incidence specular reflection using the microspectroreflectometer described elsewhere.[20] The refractive indices, calculated from the single-wavelength reflectivities using Fresnel's Law, were measured at 514.5 nm, which is the incident wavelength used in the Brillouin experiments reported here.

The previously described four-circle Brillouin scattering instrument, which allows rotation of the incident beam and sample independently so that a greater number of phonons can be sampled, was used with minimal modification.[21] This facilitates a complete determination of the stiffness tensor. Frequency shifts were measured using a triple-pass Fabry–Perot interferometer. Free spectral ranges (FSRs), were calibrated with pure liquid benzene, and ranged from 0.6 to 1.8 cm^{-1}. At least three FSRs were used for each scattering geometry using all polarization combinations, *VV*, *VH*, etc. This standard designation for polarization is used for clarity

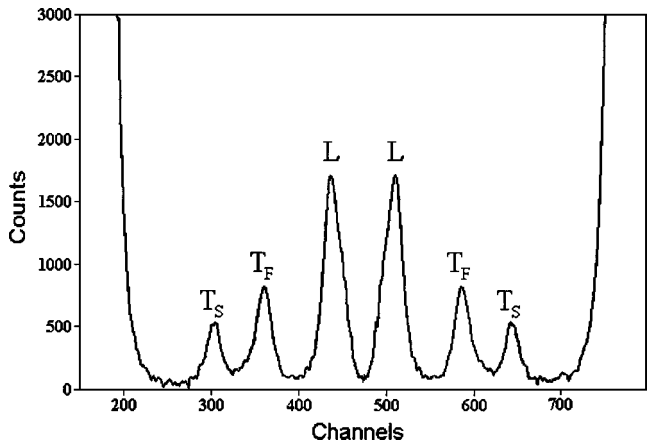

FIG. 1. *VV*-polarized Brillouin spectrum for β-HMX. Scattering is from the [0, 0.8787, −0.4772] phonon and the FSR=1.013 cm^{-1}. T_S, T_F and L denote, respectively, the slow and fast quasitransverse modes and the quasilongitudinal mode.

but the actual polarizations were along the major and minor principal directions, which were primarily vertical and horizontal, respectively, to the scattering plane. The measured Brillouin spectra are each a result of 50–200 summed interferometer scans depending on the scattering intensity of the modes observed. A representative Brillouin spectrum of β-HMX is shown in Fig. 1.

RESULTS

All 13 elastic constants for β-HMX, in standard Voigt notation,[22] are reported in Table I. The elastic constants were determined from a set of 21 velocities found from a variety of scattering geometries. Including an error of ±0.5° for angular crystal and polarization alignment, the errors in the refractive index measurement, and an error of ±0.003 cm^{-1} for determination of the acoustic-mode energy shifts, the uncertainties in the elastic constants are estimated to be on the order of 0.06 GPa. The average deviation of the experimental velocities compared to those calculated from the minimized elastic constants was 47.7 m/s or 2.4%. The largest absolute error of 10% was observed for the quasilongitudinal mode for the [001] phonon. Additionally, all principal minors of the stiffness tensor determinant were found to be positive, ensuring that the elastic constants represent a physically realistic system.[23]

TABLE I. Comparison of the elastic constants for β-HMX.

Elastic constants (GPa)	This work	Zaug[a] (Ref. 10)	Sewell *et al.* (2002) (Ref. 15)	Sewell *et al.* (2003) (Ref. 16).
C_{11}	18.41	**20.8**	19.4	22.2
C_{12}	6.37	4.8	5.9	9.6
C_{13}	10.50	12.5	8.4	13.2
C_{15}	−1.10	**−0.5**	−1.1	−0.1
C_{22}	14.41	26.9	17.5	23.9
C_{23}	6.42	5.8	8.2	13.0
C_{25}	0.83	−1.9	3.2	4.7
C_{33}	12.44	**18.5**	17.8	23.4
C_{35}	1.08	**1.9**	0.2	1.6
C_{44}	4.77	4.2	9.1	9.2
C_{46}	2.75	2.9	2.4	2.5
C_{55}	4.77	**6.1**	9.2	11.1
C_{66}	4.46	2.5	9.8	10.1

[a]"Empirically sensitive" constants appear in boldface.

The elastic constants from three other reports are also listed in Table I. In order for a valid comparison to be made to these values, the Cartesian system to which the elastic constants are referenced must be the same for all three sets. We adopt the reference system of Sewell *et al.* with the Cartesian x and y axes parallel to the a- and b-crystallographic axes, respectively, while the z axis is parallel to the reciprocal lattice vector c^*. Sewell *et al.* transformed Zaug's stiffness tensor into their reference frame, so the elastic constants in Table I, representing Zaug's experimental work as transformed by Sewell *et al.*, may be directly compared to our results and those of Sewell *et al.*

DISCUSSION

Comparison with previous experiment and theory

While a complete stiffness tensor was reported by Zaug, not all elements were completely determined by experiment. For comparison, the sound velocities, which are, respectively, calculated from the elastic constants determined in Zaug's and this work, are presented in three orthogonal planes in Fig. 2. Inspection of Fig. 2 shows that Zaug's velocities are generally larger than those found in this work. These faster velocities merely reflect that Zaug's elastic constants are generally stiffer than those determined here. However, the comparison among some elastic constants is more relevant than others. Zaug's experimental conditions most directly relate the "empirically sensitive"[10] constants, $C_{xxxx}(C_{11})$, $C_{xxxz}(C_{15})$, $C_{zzzz}(C_{33})$, $C_{zzxz}(C_{35})$ and $C_{xzxz}(C_{55})$ to his measured values. The full, four-index, tensor notation is used here to illustrate the phonon wave-vector dependence in solving the Christoffel determinant for the elastic constants. Zaug's impulse stimulated light scattering (ISLS) experiments were confined to a plane perpendicular to the y-Cartesian axis. Therefore, the elastic constants in the expanded Christoffel determinant that have an explicit association with the y-direction cosine cannot be experimentally determined from [$x0z$] phonons alone. Additionally, due to low scattering intensity or possible ambiguity in mode assignment, the quasitransverse modes were not used in Zaug's stiffness tensor minimization. Due to these experimental restrictions, the most pertinent comparison is among the five elastic constants mentioned above.

Our results show a fair agreement with Zaug's values for C_{11}, C_{33}, and C_{55} with an average difference of approximately 16%. The agreement with the off-diagonal elastic constants, C_{15} and C_{35}, is less acceptable. Traditionally, these elastic constants are the source of the greatest discrepancy.[24] For arbitrary phonon directions in low-symmetry crystals, the expanded Christoffel determinant yields a system of equations in which the elastic constants are strongly coupled to one another. Hence, as these equations become increasingly complicated, the probability for a high propagation of error grows.

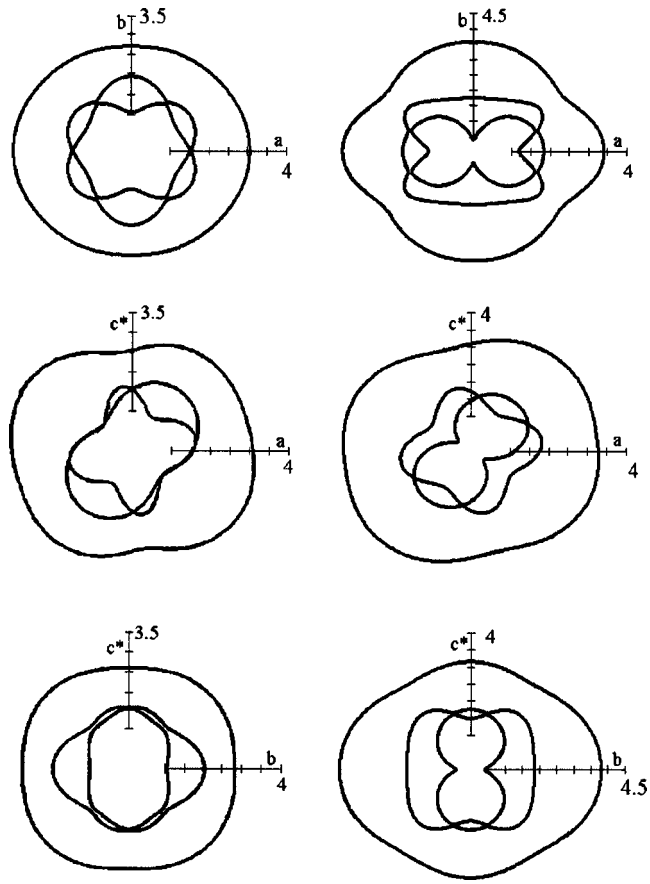

FIG. 2. Plotted sound velocities calculated from the elastic constants of this work (left) and Zaug's work (right). From the center out, each line represents the quasitransverse slow mode, quasitransverse fast mode and the quasilongitudinal mode, respectively. (Each tick mark on the abscissa and ordinate represents 0.5 km/s)

Even though ISLS and Brillouin scattering are complementary methods for elasticity measurements, fundamental differences in sample requirements provide reasons for disagreement. ISLS often requires larger crystals than those used in Brillouin scattering. These crystals are either cut or coarsely ground and subsequently polished in order to access the desired orientation. Internal defects can arise from mechanical grinding and polishing, especially for relatively soft molecular crystals. The introduced internal strain may affect the phonon dynamics. By being able to define any scattering geometry without resorting to altering the crystal itself, the Brillouin instrument used in these experiments facilitates keeping these defect-related strains to a minimum.

Although the agreement between separate elastic constants in the theoretical reports is varied, taken as a whole, the elastic constants and bulk modulus reported here are in better agreement with the earlier reported stiffness tensor of Sewell *et al.* Because of its marked difference, particular attention must be paid to the C_{22} elastic constant. Since the y-axis is parallel to the high-symmetry b-crystallograpic axis of the monoclinic lattice, C_{22} can be directly measured from the [010] phonon longitudinal mode.[17] We used a scattering geometry that directly probed this [010] phonon. Unfortunately, three modes were not observed in this spectrum. Therefore, a completely unequivocal assignment of the longitudinal mode could not be made. For reasons discussed earlier, the comparison of C_{22} with Zaug's value is uncertain.

However, the higher theoretical values prompted a reanalysis of our data. Use of a stiffer C_{22} elastic constant, comparable to that found in the second calculation by Sewell *et al.*, in the minimization routine, yielded much larger errors. This error was particularly pronounced for the velocities associated with the $[0yz]$ phonons. These spectra were used as a benchmark for accuracy for two reasons. First, as seen in Fig. 1, all three Brillouin modes were observed; therefore, a definite differentiation between the quasitransverse and quasilongitudinal modes can be made. Second, the velocities measured in symmetrically equivalent scattering geometries on three different crystals were reproducible within 1%.

Furthermore, the theoretical elastic constants are isothermal. However, the discrepancy in a direct comparison to the isentropic velocities would not produce an error of this magnitude. Our overall better agreement with the earlier reported theoretical stiffness tensor suggests that the Rahman–Parrinello *NpT* approach may be suitable for determining the elastic constants with the caveat that the theoretical potential accurately represents the system.

Although the potential used by Sewell *et al.* provided an accurate reproduction of the crystal structure and lattice energy, this does not necessarily guarantee that the curvature of the potential's hypersurface accurately represents the elasticity.[25] Theoretical elastic constants are often stiffer compared to those of experiment. This overestimation is usually attributed to the use of the rigid-body approximation for flexible molecules or to neglecting the anharmonic softening of the lattice with temperature. Our more compliant C_{22} value may also be partly explained by an acoustic damping via coupling to low-energy molecular modes.[26] This is relevant to the "doorway mode" anharmonic coupling model that has been posited by Dlott and Fayer to be an important feature of detonation of secondary explosives.[27] Experimental and theoretical vibrational analyses of β-HMX have shown the presence of low-energy modes that have the necessary symmetry for coupling.[28–30] However, a lack of consistency in the assignment of these modes to either the molecular or lattice regime precludes an exact analysis of this coupling without further experimental investigation.

The theoretical works of Sewell *et al.* use a fully flexible molecular potential that begins to account for anharmonicity. However, ascertaining how accurately a given potential mimics the real system requires comparison to experiment. Beyond augmenting theoretical potentials, independent experimental stiffness tensor determinations also begin to mitigate the experimental errors associated with determining elastic constants. This allows for the development of a more consistent stiffness tensor, particularly, for the case of lower-symmetry crystals.[25] Therefore, an individual elastic constant comparison to theory would be more insightful after a thorough experimental basis, including pressure- and temperature-dependent studies, has been developed.

TABLE II. Bulk (K) and shear moduli (G) for β-HMX.

Modulus[a] (GPa)	This work	Zaug (Ref. 10)	Sewell *et al.* (2002) (Ref. 15)	Sewell *et al.* (2003) (Ref. 16)
K_V	10.2	12.5	11.1	15.7
K_R	9.6	12.5	10.9	15.1
K_{VRH}	9.9	12.5	11.0	15.4
G_V	4.3	5.4	7.8	8.3
G_R	3.1	1.3	6.7	7.0
G_{VRH}	3.7	3.4	7.3	7.7

[a]V, R, and VRH denote, respectively, the moduli calculated using the Voigt, Reuss, and Voigt–Reuss–Hill approximation.

Bulk and shear moduli

Previous experimental and theoretical isotherms have been used to calculate isothermal bulk moduli ranging from 9 GPa to almost 17 GPa.[16,31,32] For comparison, the approximation that the isothermal and adiabatic moduli are nearly the same under ambient conditions is made. The Reuss (K_R) and Voigt (K_V) bulk moduli were calculated using[33]

$$K_R = \left(\sum_{i,j}^{3} S_{ij}\right)^{-1}, \tag{6}$$

$$K_V = \frac{1}{9}\sum_{i,j}^{3} C_{ij}, \tag{7}$$

where S_{ij} denotes the elements of the compliance tensor. The moduli listed in Table II also include the Voigt–Reuss–Hill (VHR) arithmetic mean of K_R and K_V. Acceptable agreement is found with Zaug's experimental findings and the initial theoretical work of Sewell *et al.* While our results suggest the bulk modulus is lower than recently reported,[16,31,32] the possibility of a larger modulus is certainly not without precedent. However, Sewell *et al.* have shown that the analysis of compression isotherms using different equations of state can yield results varying as much as 5 GPa within a given data set.[16,34] This variance is, in part, due to the higher curvature of an isotherm at lower pressures. Therefore, a complementary method for determining the bulk modulus at strictly ambient pressure is required. The complete stiffness tensor reported here provides such an experimental determination.

Analogous to the association of a higher bulk modulus to lower hydrostatic compressibility, the shear modulus relates to resistance in shearing. Since shear deformations have been proposed to be a critical component in the initiation of detonation,[35–37] a precise determination of the shear modulus is necessary for substantiating possible detonation mechanisms. The Reuss (G_R) and Voigt (G_V) shear moduli for β-HMX were calculated using[33]

$$G_R = \left[\tfrac{4}{15}(s_{11}+s_{22}+s_{33}) - \tfrac{4}{15}(s_{12}+s_{13}+s_{23}) + \tfrac{1}{5}(s_{44}+s_{55}+s_{66})\right]^{-1}, \tag{8}$$

$$G_V = \tfrac{1}{15}(c_{11}+c_{22}+c_{33}) - \tfrac{1}{15}(c_{12}+c_{13}+c_{23}) + \tfrac{1}{5}(c_{44}+c_{55}+c_{66}). \tag{9}$$

These shear moduli, along with the VHR average, are shown in Table II. Good agreement is found between the shear moduli calculated from two experimental works, while the theoretical moduli were almost twice that determined from experiment. This suggests that β-HMX has a decreased resistance to shear than theoretically predicted.

Physical interpretation

Since the consistency amongst the reported stiffness tensors is limited, the interpretation of other physical phenomena can also provide supporting evidence for the reported elasticity values. Cleavage planes have been previously used to substantiate the presence of weak intermolecular forces.[38] A classic example of this association is seen in graphite. While hexagonal sheets of covalently bonded carbon act as an exaggeration of "intermolecular bonding" when compared to forces connecting separate sheets, the logic may be extended to van der Waals crystals. The two elastic constants C_{11} and C_{22}, which are directly associated with the forces within the graphite sheets, are on the order of 1000 GPa.[39] In comparison, the C_{33} elastic constant, which relates to the weak forces disrupted as carbon sheets are separated, is approximately 40 GPa. While the relation of elastic constants and cleavage planes becomes less distinct for traditional molecular crystals, its application to systems such as anthracene and phenothiazine warrants its use here.[24,38] The observation of a (011) cleavage plane in β-HMX by Palmer and Field[40] suggests that the intermolecular forces in the bc^* plane are weaker. This observation is supported by the lower C_{22} and C_{33} elastic constants compared to C_{11}.

While cleavage planes may be qualitatively related to single elastic constants, other macroscopic observations are more realistically associated with the entire tensor. The linear compressibility relates a relative change in a linear dimension to an applied hydrostatic pressure. The linear compressibility is calculated from

$$\beta = \sum_i \sum_j s_{ijkk} q_i q_j. \tag{10}$$

In general, the compressibility is a function of direction and can provide insight into the anisotropy in the strength of intermolecular interactions. Thus, a direction in which the intermolecular interactions are stronger would reflect a lower compressibility in that direction. A polar plot of Eq. (10) provides an association of the entire compliance tensor and compressibility which more accurately portrays the tensor property rather than using single elements of the tensor that have a greater projection along a given direction. The compressibilities of β-HMX and respective crystallographic projections, plotted in three orthogonal planes, are presented in Fig. 3. These plots show directions of lower compressibility which is particularly evident along the a axis. Also, the average compressibility is greater in the bc^* crystallographic plane than in either the ac^* or ab plane. This suggests that the intermolecular interactions are weaker in this plane

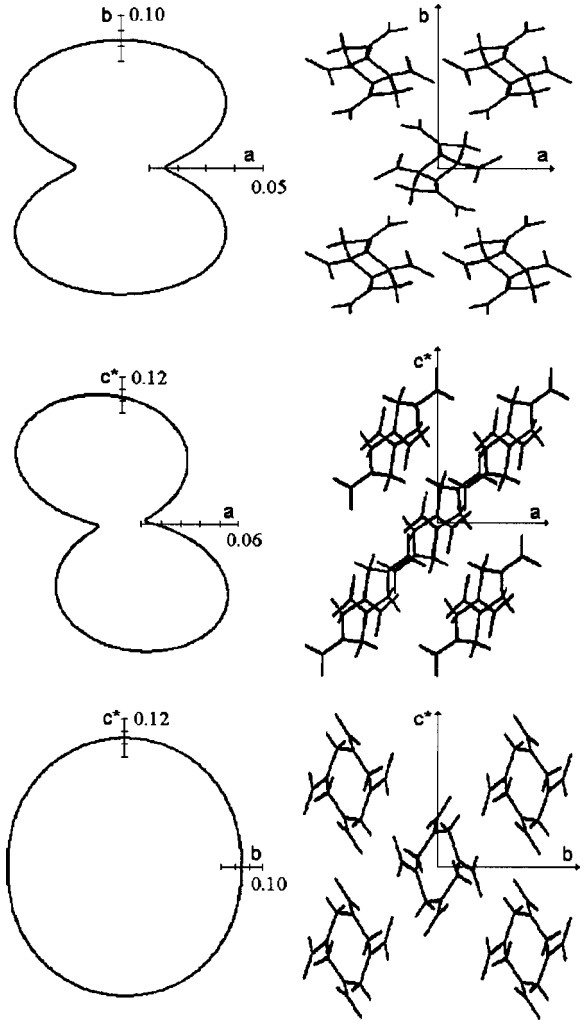

FIG. 3. Linear compressibility diagrams and crystallographic projections for β-HMX. (Each tick mark on the abscissa and ordinate in the linear compressibility plots represents 0.01 GPa^{-1})

which further correlates to the [011] cleavage plane.

Patterns in crystal growth can also provide information about the microscopic interactions and how they manifest themselves in the solid state. The observations that crystals of β-HMX are zonal to the crystallographic *a* axis and elongated along it suggest that the intermolecular interactions are stronger along this direction. This qualitatively substantiates C_{11} as being the largest elastic constant. This qualitative association can be observed for a variety of molecular crystals that exhibit a definite zonal axis.[41] Additionally, the single-crystal x-ray diffraction study by Kohno *et al.* shows that there are shorter hydrogen-bonded contacts along the *a* axis, which may stiffen the associated C_{11} elastic constant. These short contacts reflect a stronger intermolecular interaction which is consistent with the decreased compressibility, as well as the larger sound velocities, in this direction. The observations of the macroscopic behavior of β-HMX suggest that the relative ordering of the first three diagonal elastic constants should be $C_{11} > C_{22} \sim C_{33}$. This ordering is observed in this work as well as that initially calculated by Sewell *et al.*

While intermolecular forces are more difficult to directly interpret from the shear elastic constants, some insight can be gained by examining their deviation from Cauchy behavior which assumes (1) all constituent molecules are at sites of inversion and (2) the forces connecting two points is purely a function of distance, i.e., a central potential. Under this approximation, the deduced Cauchy relations—$C_{12}=C_{66}$, $C_{13}=C_{55}$, $C_{23}=C_{44}$, and $C_{25}=C_{46}$—decrease the number of independent elastic constants for a monoclinic system from 13 to 9.[42] For our stiffness tensor, the average deviation from a purely central-force approximation is about 44%. While the C_i site symmetry of β-HMX fulfills the requirement of inversion, the large percent deviation suggests the importance of many-body interactions in accurately describing β-HMX. These angular and torsional interactions may be an expected consequence of the high number of flexible nitrogroups.

Relevance to detonation

During the *initial* excitation by a shockwave, the lattice, although greatly deformed, remains intact. Furthermore, it is arguable that the elastic constants for the *initially* shock-compressed medium can be approximated by the equilibrium lattice values since there is insufficient time for renormalization to new values. Therefore, the mechanical properties are crucial for understanding this initial deformation, as well as how the deformation energy couples from the lattice into the molecular degrees of freedom. Some of the previously developed models for detonation have introduced a correlation between shear strain and detonation. Orientationally sensitive detonation was observed in pentaerythritol tetranitrate (PETN).[36] The proposed argument for this detonation anisotropy was that interleaving molecules of PETN "sterically hindered" particular slip systems activated by the uniaxial compression of the shockwave.[37] Those slip systems that were most hindered were associated with directions that were most sensitive to detonation. However, the fundamental question of how energy coupled into the molecular degrees of freedom for bond dissociation remained unanswered. Gilman has proposed that the extreme shear-induced deformation of the molecule's electron density results in local "metallization", i.e., a closure of the highest-occupied-molecular-orbital–lowest-occupied-molecular-orbital (HOMO-LUMO) gap.[35] A model for mechanochemical transformations based on this idea has been proposed by Luty *et al.*[43] This model defines a deformation energy ϕ_{def} that quantifies the mechanically induced decrease in the HOMO–LUMO gap and shows that complete band-gap closure is unnecessary for reaction. Since ϕ_{def} is intimately associated with the dynamical matrix, elasticity measurements are required to quantify its role in detonation. Additionally, shear deformation provides a symmetry-breaking distortion of the molecule. This decrease in symmetry is proposed by Luty *et al.* to facilitate a coupling to the electronic states of the molecule and formation of subsequent chemical reactions.

While a detailed understanding of elasticity's role in the initiation of detonation is limited by a lack of experimental evidence, the stiffness tensor for β-HMX provides an initial substantiation of the importance of shear in detonation. Although the relationship between stress and strain involves the

entire stiffness tensor, specific interactions can be associated, to a degree, with the appropriate elastic constants. The shorter intermolecular O–H contacts along the *a* axis may facilitate a shear-induced dislocation along the other crystallographic directions. Since the nitrogroups contribute to the interactions that stiffen the *a* axis, a shear dislocation may distort the molecule such that the $N–NO_2$ bond suffers a pronounced deformation. This bond, at least for nitramine explosives, is suspected to be the initial bond fractured in detonation and has been shown by calculation to specifically occur for cyclotrimethylenetrinitramine (RDX).[43–45]

Using the linear elasticity of β-HMX, one may speculate on a similar detonation anisotropy seen in PETN. While the cyclic β-HMX molecule precludes a strong interleaving of molecular contacts, the shorter molecular interactions along the *a* axis may provide an analogous situation to the sterically hindered slip systems in PETN. Therefore, the shockwave compression that more markedly affects these stronger interactions may be associated with a direction of higher detonation sensitivity. However, much additional work will be required before such a connection can be justified. While the subsequent shockwave-induced lattice deformation may be necessarily plastic, the elasticity provides crucial insight into the initial molecular deformation and its relation to the initial step in the mechanism of detonation.

CONCLUSION

Brillouin scattering from a variety of acoustic phonons propagating in orthogonal planes allowed the experimental determination of all 13 elastic constants of β-HMX. Comparison to previously reported stiffness tensors produced a varied agreement. Three of the five "empirically sensitive" elastic constants determined by Zaug correlated fairly well with results presented here. The earlier reported theoretical elastic constants by Sewell *et al.* agree better with our results than did their later calculation. Our more compliant stiffness tensor indicates that effects of anharmonicity are more important than suggested by recent calculations. The low-pressure determination of the adiabatic bulk modulus is found to be 9.9 GPa. Precise determinations of this elastic tensor's invariant at low pressures are required for its application in equations of state. With an improving experimental basis for comparison, further progress in the theoretical modeling of high explosives can be realized.

Intermolecular forces associated with the observed (011) cleavage plane are qualitatively used to corroborate the relative ordering of C_{11}, C_{22} and C_{33}. This observation is further substantiated by patterns in crystal growth and molecular packing. Additional information about intermolecular forces is garnered from the observed deviation from Cauchy behavior. This deviation suggests a higher degree of elastic anisotropy that may necessitate the role of many-body interactions in describing β-HMX.

The stiffness tensor of β-HMX shows compliant *b* and *c* axes, which favor dislocations along these directions. Recently reported mechanisms for detonation suggest that a strong shear deformation is integral to understanding how mechanical energy is initially transferred into the molecule.[35,37,43] Undoubtedly, as the mechanical properties of high explosives become more widely quantified, a broader understanding of the initial mechanism for detonation can be gained.

ACKNOWLEDGMENTS

Support of this research by the U.S. Office of Naval Research under Grant No. N000149810736 and by Pfizer, Inc. is gratefully acknowledged.

[1] T. Luty and C. J. Eckhardt, in *Cooperative Effects in Solid-State Reactions*, Reactivity of Molecular Solids, in Molecular Solid State, Vol. No. 3, edited by E. Boldyreva and V. Boldyrev (Wiley, Chichester, 1999), Chap. 2.
[2] H. Iwahura, T. Sugawara, K. Itoh, and T. Takui, Mol. Cryst. Liq. Cryst. **125**, 251 (1985).
[3] O. Ermer, J. Am. Chem. Soc. **110**, 3747 (1988).
[4] G. M. J. Schmidt, in *Solid State Chemistry*, edited by D. Ginsburg (Verlag, Weinheim, Germany, 1976), p. 2.
[5] J. M. McBride, B. E. Segmuller, M. D. Hollingsworth, D. E. Mills, and B. A. Weber, Science **234**, 830 (1986).
[6] N. M. Peachey and C. J. Eckhardt, J. Phys. Chem. **97**, 10849 (1993).
[7] P. Maffre and M. Peyrard, J. Phys.: Condens. Matter **6**, 4869 (1994).
[8] C. S. Choi and H. P. Boutin, Acta Crystallogr., Sect. B: Struct. Crystallogr. Cryst. Chem. **B26**, 1235 (1970).
[9] Y. Kohno, K. Maekawa, N. Azuma, T. Tsuchioka, T. Hashizume, and A. Imamura, Kogyo Kayaku **53**, 227 (1992).
[10] J. M. Zaug, *Proceedings of the 11th Detonation Symposium*, 1998 (unpublished), p. 498.
[11] S. Ye, K. Tonokura, and M. Koshi, Kayaku Gakkaishi **63**, 104 (2002).
[12] D. C. Sorescu, B. M. Rice, and D. L. Thompson, J. Phys. Chem. A **102**, 8386 (1998).
[13] A. V. Dzyabchenko, T. S. Pivina, and E. A. Arnautova, J. Mol. Struct. **378**, 67 (1996).
[14] J. P. Lewis, T. D. Sewell, R. B. Evans, and G. A. Voth, J. Phys. Chem. B **104**, 1009 (2000).
[15] T. D. Sewell, D. Bedrov, R. Menikoff, and G. D. Smith, in *Shock Compression of Condensed Matter*, AIP Conf. Proc.No. 620 (AIP, New York, 2002), Part 1, p. 399.
[16] T. D. Sewell, R. Menikoff, D. Bedrov, and G. D. Smith, J. Chem. Phys. **119**, 7418 (2003).
[17] H. Z. Cummins and P. E. Schoen, in *Laser Handbook*, edited by F. T. Arecchi and E. O. Schulz-Dubois (North-Holland, Amsterdam, 1972), Chap. El.
[18] I. L. Fabelinskii, *Molecular Scattering of Light* (Plenum, New York, 1968).
[19] K. H. Brose, and C. J. Eckhardt, Chem. Phys. Lett. **125**, 235 (1986).
[20] C. J. Eckhardt, and R. R. Pennelly, Chem. Phys. Lett. **9**, 572 (1971).
[21] R. C. Dye, J. Sartwell, and C. J. Eckhardt, Rev. Sci. Instrum. **60**, 2610 (1989).
[22] J. F. Nye, *Physical Properties of Crystals* (University Press, London, 1957).
[23] M. Born, and K. Huang, *Dynamical Theory of Lattices* (Oxford University Press, Oxford, 1954).
[24] R. C. Dye, and C. J. Eckhardt, J. Chem. Phys. **90**, 2090 (1989).
[25] G. M. Day, S. L. Price, and M. Leslie, Cryst. Growth Des. **1**, 13 (2001).
[26] L. N. Liebermann, in *Physical Acoustics*, edited by W. P. Mason (Academic, New York, 1966) Vol. 4.
[27] D. D. Dlott, and M. D. Fayer, J. Chem. Phys. **92**, 3798 (1990).
[28] Z. Iqbal, S. Bulusa, and J. R. Autera, J. Chem. Phys. **60**, 221 (1974).
[29] F. Goetz, and T. B. Brill, J. Phys. Chem. **83**, 340 (1979).
[30] H. V. Brand, R. L. Rabie, D. J. Funk, I. Diaz-Acosta, P. Pulay, and T. K. Lippert, J. Phys. Chem. B **106**, 10594 (2002).
[31] B. Olinger, B. Roof, and H. Cady, Proceedings of the Symposium (Intern.) On High Dynamic Pressures C. E. A., Paris, France, 1978 (unpublished), p. 3.
[32] C.-S. Yoo and H. Cynn, J. Chem. Phys. **111**, 10229 (1999).
[33] E. Schreiber, O. L. Anderson, and N. Soga, *Elastic Constants and Their Measurement* (McGraw-Hill, New York, 1973). Equation 2.22, p. 30, of this reference omitted the factor of (1/15). This was subsequently corrected in Eq. (8) of this manuscript.

[34]R. Menikoff, and T. D. Sewell, High Press. Res. **21**, 121 (2001).
[35]J. J. Gilman, Philos. Mag. B **71**, 1057 (1995).
[36]J. J. Dick, Appl. Phys. Lett. **44**, 859 (1984).
[37]J. J. Dick, and J. P. Ritchie, J. Appl. Phys. **76**, 2726 (1994).
[38]J. Sartwell, and C. J. Eckhardt, Phys. Rev. B **48**, 12438 (1993).
[39]O. L. Blakslee, D. G. Proctor, E. J. Seldrin, G. B. Spence, and T. Weng, J. Appl. Phys. **41**, 3373 (1970).
[40]S. J. P. Palmer, and J. E. Field, Proc. R. Soc. London, Ser. A **383**, 399 (1982).
[41]S. Haussuhl, Z. Kristallogr. **216**, 339 (2001).
[42]A. E. H. Love, *The Mathematical Theory of Elasticity*, 4th ed. (Cambridge University Press, London, 1934).
[43]T. Luty, P. Ordon, and C. J. Eckhardt, J. Chem. Phys. **117**, 1775 (2002).
[44]M. Choi, H. Kim, and C. J. Chung, J. Phys. Chem. **99**, 15785 (1995).
[45]T. R. Botcher, and C. A. Wright, J. Phys. Chem. **97**, 9149 (1993).